

Structure of uranium(VI) oxide dihydrate, $\text{UO}_3 \cdot 2\text{H}_2\text{O}$; synthetic *meta*-schoepite $(\text{UO}_2)_4\text{O}(\text{OH})_6 \cdot 5\text{H}_2\text{O}$

Mark. T. Weller,* Mark E. Light
and Thomas Gelbrich

Department of Chemistry, University of South-
ampton, Highfield, Southampton SO17 1BJ,
England

Correspondence e-mail: mtw@soton.ac.uk

The structure of uranium oxide dihydrate, also known as *meta*-schoepite $(\text{UO}_2)_4\text{O}(\text{OH})_6 \cdot 5\text{H}_2\text{O}$, has been determined from a synthetic single crystal. The structure, at 150 K, space group *Pbcn*, lattice constants $a = 14.6861$ (4), $b = 13.9799$ (3) and $c = 16.7063$ (5) Å, consists of layers of stoichiometry $(\text{UO}_2)_4\text{O}(\text{OH})_6$, formed from edge-sharing UO_7 pentagonal bipyramids, interleaved with hydrogen-bonded water molecules. Three of the layer hydroxyl groups are linked through hydrogen bonding to single water molecules and the three remaining OH units form interactions with water molecules that each act as acceptors in two hydrogen bonds. One of the water molecules in the inter-layer region is disordered over two symmetry-related sites and forms hydrogen-bonded interactions only within the layer and with the uranyl O atoms. The relationship of the structure of *meta*-schoepite to that of schoepite is discussed in detail.

Received 28 July 1999

Accepted 20 December 1999

1. Introduction

The chemistry of the hydrated oxides of uranium(VI) is extremely complex and approximately 20 such phases have been described. All the structures of these materials are based on polyhedral sheets of the composition $(\text{UO}_2)_x(\text{O})_y(\text{OH})_z$, consisting of uranyl groups linked by oxide and hydroxide ions; for the higher hydrates these layers may be interleaved by water molecules. The structures of many of these materials have recently been described in detail by Finch *et al.* (1996) and the inter-relationships between these phases also described (Finch *et al.*, 1998).

Many of the uranium oxide hydrates occur naturally. Schoepite $[(\text{UO}_2)_8\text{O}_2(\text{OH})_{12}](\text{H}_2\text{O})_{12}$ ($= \text{UO}_3 \cdot 2.25\text{H}_2\text{O}$) was first described by Walker (1923) and subsequently investigated by many other workers (Schoep, 1932; Billet & de Jong, 1935; Christ & Clark, 1960) culminating in the full structure determination, from a naturally occurring sample, by Finch *et al.* (1996). The two related phases *para*- and *meta*-schoepite have remained less well characterized. *para*-Schoepite $\text{UO}_3 \cdot \sim 1.90\text{H}_2\text{O}$ (Schoep & Stradiot, 1947) has not been synthesized and little is known of its structure. *Meta*-schoepite may be readily synthesized using a variety of methods, but until now only in a form not suitable for full structural characterization. For example *meta*-schoepite can be obtained by the action of water on uranium oxides or alpha uranium(VI) oxide monohydrate $\text{UO}_3 \cdot 0.8\text{H}_2\text{O}$ at high temperatures (Debets & Loopstra, 1963), by precipitation from uranyl solution (Hoekstra & Siegel, 1973) and by partial dehydration of schoepite. The latter route has recently been investigated in detail by Finch *et al.* (1998). The ease of this process indicates

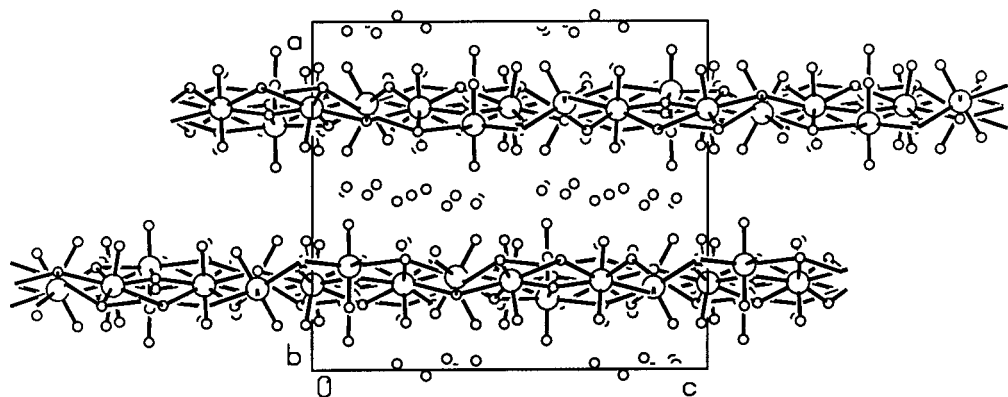


Figure 1

The structure of $(\text{UO}_2)_4\text{O}(\text{OH})_6 \cdot 5\text{H}_2\text{O}$ viewed down **b**, showing the interleaved uranium oxide hydroxide sheets and water layers.

that the two materials schoepite and *meta*-schoepite are very closely structurally related through the loss of eight molecules of water (per unit cell) from the structure, the $(\text{UO}_2)_x(\text{O})_y(\text{OH})_z$ sheets being essentially unchanged in the process. Finch *et al.* (1998) also described a likely scheme for the inter-conversion of the schoepite and *meta*-schoepite structures based on consideration of the hydrogen-bonding schemes within the schoepite structure.

The uranium oxide hydrates, as well as being of importance in the geochemistry of uranium, are also significant phases in terms of materials generated during the aqueous corrosion of uranium-based nuclear fuels. For this reason interest in the chemistry and structures of such compounds has recently been re-established. The laboratory growth of single crystals of many of these phases of a size and quality suitable for structure determination has proved impossible, until now, and most structural work has been undertaken on naturally occurring samples. Even so, the structural complexity inherent in uranium systems and the facile interconversion of one structure to another (for example, schoepite readily converts to *meta*-schoepite under the application of mechanical pressure) has proved a significant hurdle to structure elucidation. However, with the advent of high intensity X-ray sources and area detectors it has now become possible to determine structures from very small crystals, which may be the only suitable material obtainable. In this paper we describe the synthesis of single-crystal uranium(VI) oxide dihydrate (*meta*-schoepite), its structure determination by single-crystal X-ray diffraction and the relationship between the structures of schoepite and *meta*-schoepite.

2. Experimental

$\text{UO}_3 \cdot 2\text{H}_2\text{O}$, as *meta*-schoepite, was prepared using a method similar to that described originally by Hoekstra & Siegel (1973), where lanthanum hydroxide was slowly dissolved in a solution of uranyl ions in order to increase the pH to a level where precipitation just occurs. The rate of precipitation of the uranium oxide hydrate depends critically on the pH of the

solution and in order to produce single crystals of the material this needs to be set only just above the precipitation point. As lanthanum oxide slowly hydrates in contact with water this was substituted for lanthanum hydroxide in this work. 0.58 g of La_2O_3 was added to 50 ml of 0.2 M $\text{UO}_2(\text{NO}_3)_2 \cdot 6\text{H}_2\text{O}$ at room temperature. The suspension was shaken frequently over a 24 h period until the solid had fully dissolved. The resultant solution was then allowed to stand for several months in the

dark, at room temperature, over which time the product slowly crystallized. The small amount of product was highly crystalline and included numerous small tabular, hexagonal crystals of dimensions $20 \times 20 \times 1\text{--}5 \mu\text{m}$. The largest of these were selected as suitable candidates for single-crystal structural study.

3. Structure refinement

Data were collected on a Nonius Kappa CCD area-detector diffractometer at the window of a rotating anode FR591 generator (50 kV, 85 mA) using images of 1° thickness and 120 s with a detector-to-crystal distance of 50 mm ($360^\circ \varphi$ scan and ω scans to fill the Ewald sphere). Data collection and cell refinement: *Collect* (Hooft, 1998) and *Denzo* (Otwinowski & Minor, 1997); structure solution: *SHELXS97* (Sheldrick, 1990); structure refinement: *SHELXL97* (Sheldrick, 1997). All U and O atoms were located directly, with the exception of one water molecule oxygen. This final O atom, O21, was located from Fourier syntheses on a disordered site near (0.5, 0.75, 0.25), but with a significant displacement in the *z* direction. A refined site occupancy close to $\frac{1}{2}$ was obtained. Refined lattice parameters are distinctly shorter in the *b* (by 0.05 Å) and *a* (by 0.14 Å) directions compared with literature values at room temperature (Finch *et al.*, 1998) given for *meta*-schoepite, obtained by partial dehydration of schoepite, or for powdered *meta*-schoepite synthesized from solution. No attempt was made to locate the 16 hydrogen sites. Isotropic displacements only were refined for the O atoms. Details of data collection and refinement are summarized in Table 1.

4. Results

The refined atomic coordinates are summarized in Table 2 with the O atoms distinguished according to type; anisotropic displacement parameters for the U atoms are summarized in Table 3. Uranium(VI) oxide dihydrate is better represented by the formula $(\text{UO}_2)_4\text{O}(\text{OH})_6 \cdot 5\text{H}_2\text{O}$ (Figs. 1 and 2). Puckered layers of the composition $(\text{UO}_2)_4\text{O}(\text{OH})_6$ (Fig. 2) are formed

Table 1
Experimental details.

Crystal data	
Chemical formula	H ₁₆ O ₂₀ U ₄
Chemical formula weight	1288.25
Cell setting	Orthorhombic
Space group	<i>Pbcn</i>
<i>a</i> (Å)	14.6861 (4)
<i>b</i> (Å)	13.9799 (3)
<i>c</i> (Å)	16.7063 (5)
<i>V</i> (Å ³)	3429.97 (16)
<i>Z</i>	8
<i>D_x</i> (Mg m ⁻³)	4.989
Radiation type	Mo <i>K</i> α
Wavelength (Å)	0.71073
No. of reflections for cell parameters	16 680
<i>θ</i> range (°)	2.01–25.75
<i>μ</i> (mm ⁻¹)	37.752
Temperature (K)	298 (2)
Crystal form	Tablet
Crystal size (mm)	0.025 × 0.020 × 0.007
Crystal colour	Yellow
Data collection	
Diffractometer	Enraf–Nonius KappaCCD area detector
Data collection method	<i>ψ</i> and <i>θ</i> scans to fill Ewald sphere scans
Absorption correction	Empirical
<i>T_{min}</i>	0.5189
<i>T_{max}</i>	0.7780
No. of measured reflections	16 680
No. of independent reflections	3255
No. of observed reflections	2106
Criterion for observed reflections	<i>I</i> > 2σ(<i>I</i>)
<i>R_{int}</i>	0.0904
<i>θ_{max}</i> (°)	25.75
Range of <i>h, k, l</i>	−16 → <i>h</i> → 17 −12 → <i>k</i> → 17 −20 → <i>l</i> → 20
Refinement	
Refinement on	<i>F</i> ²
<i>R</i> [<i>F</i> ² > 2σ(<i>F</i> ²)]	0.0482
<i>wR</i> (<i>F</i> ²)	0.1035
<i>S</i>	0.951
No. of reflections used in refinement	3255
No. of parameters used	119
H-atom treatment	None
Weighting scheme	$w = 1/[\sigma^2(F_o^2) + (0.0470P)^2 + 0.0000P]$, where $P = (F_o^2 + 2F_c^2)/3$
(Δ/σ) _{max}	0.001
Δρ _{max} (e Å ⁻³)	2.978
Δρ _{min} (e Å ⁻³)	−2.839
Extinction method	None
Source of atomic scattering factors	<i>International Tables for Crystallography</i> (1992, Vol. C, Tables 4.2.6.8 and 6.1.1.4)

from vertex-sharing UO₇ pentagonal bipyramids in the *bc* plane; the UO₇ units in each case consist of uranyl groups (U–O 1.75–1.79 Å, O atoms O1–O8 in Table 2) oriented perpendicular to a UO₅ pentagon (U–O 2.18–2.63 Å, O atoms O9–O15 in Table 2). These layers are separated by sheets of water molecules hydrogen-bonded to themselves, the OH groups within the layers and the uranyl O atoms. Each of these features is discussed in turn.

Table 2
Fractional atomic coordinates and equivalent isotropic displacement parameters (Å²).

	$U_{eq} = (1/3)\sum_i \sum_j U^{ij} a^i a^j \mathbf{a}_i \cdot \mathbf{a}_j$			<i>U_{eq}</i>
	<i>x</i>	<i>y</i>	<i>z</i>	
U1	0.23453 (4)	0.74724 (4)	0.36301 (4)	0.01561 (18)
U2	0.29656 (5)	0.77012 (4)	0.59321 (4)	0.01655 (19)
U3	0.25426 (5)	0.51155 (4)	0.22973 (4)	0.01706 (19)
U4	0.25432 (5)	0.51460 (4)	0.50131 (4)	0.01630 (19)
O1	0.1802 (9)	0.7479 (7)	0.5935 (8)	0.032 (3)
O2	0.1438 (8)	0.4529 (7)	0.2244 (7)	0.028 (3)
O3	0.1293 (8)	0.7449 (7)	0.4127 (7)	0.026 (3)
O4	0.4167 (7)	0.7849 (7)	0.5914 (7)	0.022 (3)
O5	0.3642 (8)	0.5633 (7)	0.2359 (7)	0.026 (3)
O6	0.1416 (7)	0.5579 (7)	0.5179 (7)	0.023 (3)
O7	0.3385 (8)	0.7524 (7)	0.3101 (8)	0.034 (3)
O8	0.3692 (8)	0.4724 (7)	0.4845 (7)	0.025 (3)
O9	0.2652 (7)	0.9236 (7)	0.6079 (7)	0.019 (3)
O10	0.2028 (8)	0.3615 (6)	0.4591 (7)	0.019 (3)
O11	0.3125 (7)	0.6719 (6)	0.4737 (6)	0.016 (3)
O12	0.2152 (7)	0.5667 (7)	0.3635 (7)	0.021 (3)
O13	0.3121 (7)	0.6007 (7)	0.6270 (6)	0.019 (3)
O14	0.1846 (7)	0.6852 (7)	0.2342 (7)	0.022 (3)
O15	0.1863 (7)	0.8888 (6)	0.3066 (6)	0.018 (3)
O16	0	0.7609 (12)	1/4	0.049 (5)
O17	0.5015 (9)	0.4409 (9)	0.1386 (9)	0.048 (4)
O18	−0.0253 (10)	0.6223 (10)	0.5870 (10)	0.060 (4)
O19	0.0314 (9)	0.5621 (8)	0.3391 (8)	0.046 (4)
O20	−0.0119 (11)	0.8529 (11)	0.5792 (10)	0.081 (5)
O21	0.517 (3)	0.758 (2)	0.287 (2)	0.096 (13)

4.1. Uranium–oxygen layers

The network within the uranium oxide hydroxide layers is essentially the same as in schoepite and many other uranium(VI) complex oxides, such as fourmarierite Pb[(UO₂)₄O₃(OH)₄]·4H₂O (Piret, 1985), consisting of edge-sharing (UO₂)(O,OH)₅ pentagonal bipyramids (Fig. 3). All the O atoms in the layers form part of the hydroxyl groups, with the exception of O9 which is a three-coordinate oxide ion. The hydroxyl groups are also shared as vertices to three U(O,OH)₇, with the exception of O15 which is bridging between U1 and U2 alone.

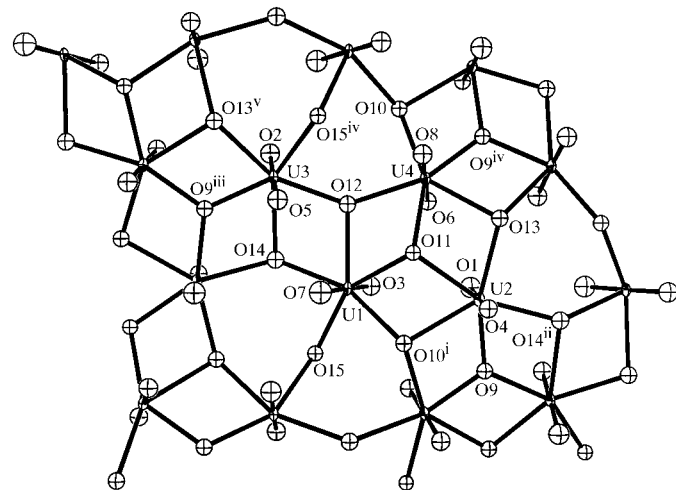


Figure 2
Part of the (UO₂)₄O(OH)₆ layer.

Table 3
Anisotropic displacement parameters ($\text{\AA}^2 \times 10^3$).

The anisotropic displacement factor exponent takes the form: $-2\pi^2[h^2a^{*2}U^{11} + \dots + 2hka^*b^*U^{12}]$.

	U^{11}	U^{22}	U^{33}	U^{23}	U^{13}	U^{12}
U1	28 (1)	14 (1)	5 (1)	-1 (1)	0 (1)	0 (1)
U2	29 (1)	13 (1)	7 (1)	-1 (1)	-1 (1)	1 (1)
U3	32 (1)	14 (1)	6 (1)	0 (1)	0 (1)	0 (1)
U4	30 (1)	13 (1)	7 (1)	1 (1)	2 (1)	-1 (1)

The linking of these units within the layer has been described in detail by Finch *et al.* (1996) and references therein. The sections of the layers not occupied by the pentagons of the UO_7 groups have a bow-tie-like motif (Fig. 3) connected centrally at the doubly bridging hydroxyl and the

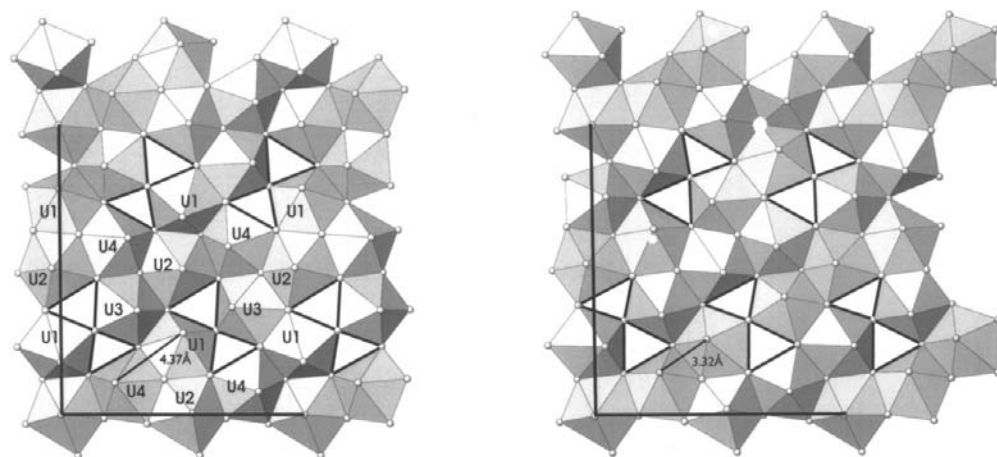


Figure 3
Comparison of the $(\text{UO}_2)_4\text{O}(\text{OH})_6$ layers in schoepite and *meta*-schoepite showing the 'bow-tie' motif. The positions of two equivalent uranyl O atoms are marked in each diagram to demonstrate the degree of change between the two structures.

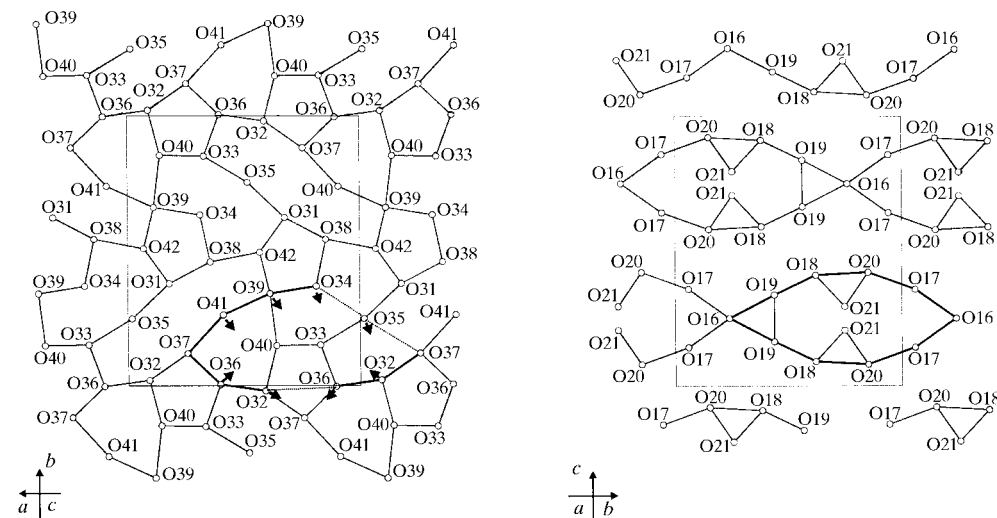


Figure 4
Comparison of the water molecule layers in schoepite and *meta*-schoepite, showing how they can be related through removal of four water molecules (shaded) per unit-cell layer and small displacements of the remaining O atoms.

Table 4
Uranium–oxygen bond lengths (\AA).

U1–O3	1.754 (12)	U2–O1	1.737 (13)
U1–O7	1.766 (13)	U2–O4	1.777 (11)
U1–O15	2.303 (9)	U2–O9	2.208 (9)
U1–O11	2.416 (10)	U2–O11	2.434 (10)
U1–O14	2.433 (11)	U2–O13	2.446 (9)
U1–O10 ⁱ	2.445 (10)	U2–O14 ⁱⁱ	2.452 (11)
U1–O12	2.540 (9)	U2–O10 ⁱ	2.578 (10)
U3–O5	1.773 (11)	U4–O6	1.784 (11)
U3–O2	1.820 (11)	U4–O8	1.810 (11)
U3–O9 ⁱⁱⁱ	2.246 (11)	U4–O9 ^{iv}	2.207 (10)
U3–O15 ^{iv}	2.315 (10)	U4–O10	2.378 (10)
U3–O12	2.433 (11)	U4–O11	2.403 (9)
U3–O13 ^v	2.475 (10)	U4–O12	2.481 (11)
U3–O14	2.636 (10)	U4–O13	2.565 (11)

Symmetry codes: (i) $-x + \frac{1}{2}, y + \frac{1}{2}, z$; (ii) $-x + \frac{1}{2}, -y + \frac{3}{2}, z + \frac{1}{2}$; (iii) $-x + \frac{1}{2}, -y + \frac{3}{2}, z - \frac{1}{2}$; (iv) $-x + \frac{1}{2}, y - \frac{1}{2}, z$; (v) $x, -y + 1, z - \frac{1}{2}$.

arrangement of these can be seen to be identical in the layers of schoepite and *meta*-schoepite (Fig. 3). The uranium–oxygen distances are summarized in Table 4 and the bond angles around uranium given in Table 5; as with schoepite, it is clear from the bond-valence calculations (Table 7) that O9 is the oxide ion and all other O atoms in this layer are part of the hydroxide ions oriented roughly perpendicular to the sheets. The bond-valence sums, using the values of Brown & Wu (1976), are reasonable for all atoms, although, as noted previously, the literature values for uranium–oxygen bond-valence parameters are generally poor at representing both the strong uranyl group and the weaker uranium–oxygen interactions. Calculations using the more recent bond-valence descriptions, for example that of Brown & Altermatt (1985), show the same trends, but with slightly modified individual values, strengthening the uranyl bonds and weakening the single uranium to oxygen bonds.

Small differences between schoepite and *meta*-schoepite exist in the orientations of the pentagonal bipyramids and specifically the directions of the UO_2 groups with respect to the

Table 5
Bond angles (°) within the (UO₂)₄O(OH)₆ sheets.

O3—U1—O7	177.8 (5)	O5—U3—O13 ^v	89.2—(4)
O3—U1—O15	86.5 (4)	O2—U3—O13 ^v	89.2 (4)
O7—U1—O15	91.5 (4)	O9 ⁱⁱⁱ —U3—O13 ^v	70.8 (3)
O3—U1—O11	92.7 (5)	O15 ^{iv} —U3—O13 ^v	77.6 (4)
O7—U1—O11	89.5 (5)	O12—U3—O13 ^v	156.7 (3)
O15—U1—O11	146.5 (3)	O5—U3—O14	88.6 (4)
O3—U1—O14	98.4 (5)	O2—U3—O14	94.0 (4)
O7—U1—O14	80.4 (5)	O9 ⁱⁱⁱ —U3—O14	66.7 (3)
O15—U1—O14	81.4 (3)	O15 ^{iv} —U3—O14	144.5 (3)
O11—U1—O14	131.6 (3)	O12—U3—O14	65.8 (3)
O3—U1—O10 ⁱ	91.9 (4)	O13 ^v —U3—O14	137.5 (3)
O7—U1—O10 ⁱ	88.6 (5)	O5—U3—U4 ^v	95.5 (4)
O15—U1—O10 ⁱ	79.9 (3)	O2—U3—U4 ^v	84.8 (4)
O11—U1—O10 ⁱ	66.6 (3)	O9 ⁱⁱⁱ —U3—U4 ^v	30.3 (2)
O14—U1—O10 ⁱ	158.0 (3)	O15 ^{iv} —U3—U4 ^v	118.8 (3)
O3—U1—O12	83.2 (4)	O12—U3—U4 ^v	160.9 (2)
O7—U1—O12	98.0 (4)	O13 ^v —U3—U4 ^v	41.4 (2)
O15—U1—O12	145.1 (4)	O14—U3—U4 ^v	96.7 (2)
O11—U1—O12	67.5 (3)	O5—U3—U2 ⁱⁱⁱ	83.6 (4)
O14—U1—O12	67.4 (3)	O2—U3—U2 ⁱⁱⁱ	98.9 (4)
O10 ⁱ —U1—O12	133.5 (3)	O9 ⁱⁱⁱ —U3—U2 ⁱⁱⁱ	29.1 (2)
O3—U1—U2	75.2 (4)	O15 ^{iv} —U3—U2 ⁱⁱⁱ	168.9 (3)
O7—U1—U2	106.5 (4)	O12—U3—U2 ⁱⁱⁱ	104.2 (2)
O15—U1—U2	113.5 (3)	O13 ^v —U3—U2 ⁱⁱⁱ	99.0 (2)
O11—U1—U2	35.3 (2)	O14—U3—U2 ⁱⁱⁱ	38.5 (2)
O14—U1—U2	162.9 (2)	U4 ^v —U3—U2 ⁱⁱⁱ	59.353 (15)
O10 ⁱ —U1—U2	39.1 (2)	O5—U3—U1	72.3 (3)
O12—U1—U2	95.9 (3)	O2—U3—U1	109.5 (4)
O3—U1—U3	108.2 (3)	O9 ⁱⁱⁱ —U3—U1	99.4 (2)
O7—U1—U3	72.0 (3)	O15 ^{iv} —U3—U1	109.3 (3)
O15—U1—U3	120.2 (3)	O12—U3—U1	37.6 (2)
O11—U1—U3	91.9 (2)	O13 ^v —U3—U1	159.4 (2)
O14—U1—U3	40.0 (2)	O14—U3—U1	36.4 (2)
O10 ⁱ —U1—U3	151.5 (2)	U4 ^v —U3—U1	129.40 (2)
O12—U1—U3	35.8 (3)	U2 ⁱⁱⁱ —U3—U1	70.394 (17)
U2—U1—U3	126.269 (19)	O6—U4—O8	179.2 (5)
O3—U1—U4	77.0 (3)	O6—U4—O9 ^{iv}	87.1 (4)
O7—U1—U4	105.0 (3)	O8—U4—O9 ^{iv}	93.4 (4)
O15—U1—U4	163.2 (3)	O6—U4—O10	93.2 (4)
O11—U1—U4	33.8 (2)	O8—U4—O10	87.6 (4)
O14—U1—U4	104.1 (2)	O9 ^{iv} —U4—O10	71.3 (4)
O10 ⁱ —U1—U4	97.1 (2)	O6—U4—O11	92.8 (4)
O12—U1—U4	36.7 (3)	O8—U4—O11	86.4 (4)
U2—U1—U4	59.246 (14)	O9 ^{iv} —U4—O11	136.7 (4)
U3—U1—U4	69.231 (16)	O10—U4—O11	151.6 (4)
O1—U2—O4	176.3 (5)	O6—U4—O12	80.2 (4)
O1—U2—O9	88.2 (4)	O8—U4—O12	99.6 (5)
O4—U2—O9	95.5 (4)	O9 ^{iv} —U4—O12	152.5 (4)
O1—U2—O11	89.7 (5)	O10—U4—O12	85.2 (3)
O4—U2—O11	87.5 (4)	O11—U4—O12	68.6 (3)
O9—U2—O11	131.3 (4)	O6—U4—O13	91.2 (4)
O1—U2—O13	85.3 (4)	O8—U4—O13	88.4 (4)
O4—U2—O13	91.4 (4)	O9 ^{iv} —U4—O13	69.7 (3)
O9—U2—O13	159.2 (4)	O10—U4—O13	140.4 (3)
O11—U2—O13	68.5 (3)	O11—U4—O13	67.1 (3)
O1—U2—O14 ⁱⁱ	98.9 (5)	O12—U4—O13	134.3 (3)
O4—U2—O14 ⁱⁱ	82.8 (5)	O6—U4—U2 ^{iv}	93.4 (3)
O9—U2—O14 ⁱⁱ	70.7 (4)	O8—U4—U2 ^{iv}	87.3 (3)
O11—U2—O14 ⁱⁱ	157.0 (3)	O9 ^{iv} —U4—U2 ^{iv}	30.1 (3)
O13—U2—O14 ⁱⁱ	90.8 (3)	O10—U4—U2 ^{iv}	41.5 (3)
O1—U2—O10 ⁱ	95.4 (5)	O11—U4—U2 ^{iv}	164.8 (3)
O4—U2—O10 ⁱ	85.6 (4)	O12—U4—U2 ^{iv}	126.2 (2)
O9—U2—O10 ⁱ	67.4 (3)	O13—U4—U2 ^{iv}	98.9 (2)
O11—U2—O10 ⁱ	64.3 (3)	O6—U4—U3 ^{vi}	83.0 (4)
O13—U2—O10 ⁱ	132.8 (3)	O8—U4—U3 ^{vi}	97.1 (4)
O14 ⁱⁱ —U2—O10 ⁱ	135.1 (3)	O9 ^{iv} —U4—U3 ^{vi}	30.9 (3)
O1—U2—U4 ⁱ	88.2 (3)	O10—U4—U3 ^{vi}	102.1 (3)
O4—U2—U4 ⁱ	94.8 (3)	O11—U4—U3 ^{vi}	106.2 (2)
O9—U2—U4 ⁱ	30.1 (3)	O12—U4—U3 ^{vi}	162.0 (2)
O11—U2—U4 ⁱ	101.2 (2)	O13—U4—U3 ^{vi}	39.6 (2)
O13—U2—U4 ⁱ	167.8 (3)	U2 ^{iv} —U4—U3 ^{vi}	60.965 (16)
O14 ⁱⁱ —U2—U4 ⁱ	100.4 (2)	O6—U4—U2	77.2 (3)
O10 ⁱ —U2—U4 ⁱ	37.7 (2)	O8—U4—U2	102.1 (3)

Table 5 (continued)

O1—U2—U3 ⁱⁱ	87.1 (4)	O9 ^{iv} —U4—U2	103.2 (3)
O4—U2—U3 ⁱⁱ	96.3 (3)	O10—U4—U2	169.3 (3)
O9—U2—U3 ⁱⁱ	29.6 (3)	O11—U4—U2	35.8 (2)
O11—U2—U3 ⁱⁱ	160.7 (2)	O12—U4—U2	97.6 (2)
O13—U2—U3 ⁱⁱ	130.1 (3)	O13—U4—U2	37.1 (2)
O14 ⁱⁱ —U2—U3 ⁱⁱ	42.0 (2)	U2 ^{iv} —U4—U2	133.30 (3)
O10 ⁱ —U2—U3 ⁱⁱ	97.0 (2)	U3 ^{vi} —U4—U2	72.447 (18)
U4 ⁱ —U2—U3 ⁱⁱ	59.682 (16)	O6—U4—U1	75.3 (3)
O1—U2—U4	71.6 (3)	O8—U4—U1	104.1 (3)
O4—U2—U4	104.8 (3)	O9 ^{iv} —U4—U1	157.7 (3)
O9—U2—U4	153.1 (3)	O10—U4—U1	122.5 (3)
O11—U2—U4	35.3 (2)	O11—U4—U1	34.0 (2)
O13—U2—U4	39.3 (3)	O12—U4—U1	37.7 (2)
O14 ⁱⁱ —U2—U4	128.6 (2)	O13—U4—U1	96.6 (2)
O10 ⁱ —U2—U4	96.4 (2)	U2 ^{iv} —U4—U1	160.95 (2)
U4 ⁱ —U2—U4	128.62 (2)	U3 ^{vi} —U4—U1	130.73 (2)
U3 ⁱⁱ —U2—U4	155.78 (2)	U2—U4—U1	59.933 (15)
O1—U2—U1	76.2 (4)	U4 ⁱ —O9—U2	119.8 (5)
O4—U2—U1	102.8 (4)	U4 ⁱ —O9—U3 ⁱⁱ	118.8 (4)
O9—U2—U1	98.0 (3)	U2—O9—U3 ⁱⁱ	121.3 (5)
O11—U2—U1	35.0 (2)	U4—O10—U1 ^{iv}	131.5 (5)
O13—U2—U1	99.6 (3)	U4—O10—U2 ^{iv}	100.8 (4)
O14 ⁱⁱ —U2—U1	168.0 (2)	U1 ^{iv} —O10—U2 ^{iv}	104.2 (3)
O10 ⁱ —U2—U1	36.7 (2)	U4—O11—U1	112.2 (4)
U4 ⁱ —U2—U1	68.745 (17)	U4—O11—U2	108.9 (4)
U3 ⁱⁱ —U2—U1	126.09 (2)	U1—O11—U2	109.7 (4)
U4—U2—U1	60.820 (15)	U3—O12—U4	134.8 (4)
O5—U3—O2	177.3 (5)	U3—O12—U1	106.6 (4)
O5—U3—O9 ⁱⁱⁱ	90.2 (5)	U4—O12—U1	105.6 (4)
O2—U3—O9 ⁱⁱⁱ	91.4 (5)	U2—O13—U3 ^{vi}	137.9 (5)
O5—U3—O15 ^{iv}	85.8 (4)	U2—O13—U4	103.6 (4)
O2—U3—O15 ^{iv}	91.7 (4)	U3 ^{vi} —O13—U4	99.0 (3)
O9 ⁱⁱⁱ —U3—O15 ^{iv}	148.2 (4)	U1—O14—U2 ⁱⁱⁱ	136.4 (4)
O5—U3—O12	91.8 (5)	U1—O14—U3	103.7 (4)
O2—U3—O12	88.7 (5)	U2 ⁱⁱⁱ —O14—U3	99.4 (4)
O9 ⁱⁱⁱ —U3—O12	132.4 (3)	U1—O15—U3 ⁱ	138.4 (5)
O15 ^{iv} —U3—O12	79.3 (3)		

Symmetry codes: (i) $-x + \frac{1}{2}, y + \frac{1}{2}, z$; (ii) $-x + \frac{1}{2}, -y + \frac{3}{2}, z + \frac{1}{2}$; (iii) $-x + \frac{1}{2}, -y + \frac{3}{2}, z - \frac{1}{2}$; (iv) $-x + \frac{1}{2}, y - \frac{1}{2}, z$; (v) $x, -y + 1, z - \frac{1}{2}$; (vi) $x, -y + 1, z + \frac{1}{2}$; (vii) $-x + 1, y, -z + \frac{1}{2}$.

layers. For example in Fig. 3, the positions of two of the On atoms on one U atom as marked are tilted towards each other in *meta*-schoepite, but away from each other in schoepite. This results from the differences in the distributions of the inter-leaving water molecules which hydrogen bond to the uranyl units. In schoepite the number of hydroxide groups in (UO₂)₄O(OH)₆ is equivalent to the number of water molecules between the layers and consequently each hydroxide is strongly hydrogen-bonded to a different water molecule. In *meta*-schoepite, (UO₂)₄O(OH)₆·5H₂O, with one less water molecule in the formula unit there are insufficient water molecules to form links with all the hydroxide ions on a 1:1 basis. By consideration of the oxygen (hydroxide ions) to oxygen (water molecules; Table 6) distances it can be seen that two water molecules O16W and O17W both have two interactions with hydroxide groups in different layers. O16W, which is sited on the higher symmetry fourfold site, interacts with two O14(H) and O17W interacts with O13(H) and O15(H). The nature of these interactions agrees well with the bond-valence scheme presented for the hydroxyl O atoms in Table 7. The weakest U—O link (bond-valence sum, b.v.s., 0.95) occurs for O14, presumably because this has a stronger OH bond as the acceptor water molecule O16 performs this

Table 6

Potential hydrogen bonding O...O contacts (Å) to 34 Å for the uranyl O atoms O1–O8, the hydroxyl O atoms O10–O15 and the water O atoms O16–O21.

O1–O21 ^{vii}	3.12 (4)	O16–O3 ^{viii}	3.324 (12)
O1–O20	3.19 (2)	O16–O3	3.324 (12)
O2–O19	2.954 (18)	O17–O8 ^{xi}	2.833 (18)
O2–O19 ^{viii}	3.174 (17)	O17–O13 ^v	2.849 (17)
O2–O21 ^{ix}	3.30 (4)	O17–O15 ^{xiv}	2.955 (17)
O3–O19	3.180 (16)	O17–O20 ⁱⁱⁱ	3.052 (19)
O3–O16	3.324 (12)	O17–O5	3.104 (17)
O4–O19 ^x	2.959 (16)	O17–O16 ^{xiv}	3.130 (18)
O4–O18 ^x	3.360 (19)	O17–O5 ^{xi}	3.348 (17)
O4–O16 ⁱⁱ	2.987 (12)	O18–O10 ^{xii}	2.727 (18)
O5–O17	3.104 (17)	O18–O21 ^{vii}	2.77 (4)
O5–O21 ^{xi}	3.26 (4)	O18–O19 ^{xii}	2.860 (18)
O5–O17 ^{xi}	3.348 (17)	O18–O7 ^{vii}	3.167 (19)
O6–O18	2.855 (18)	O18–O20	3.23 (2)
O6–O19	3.397 (18)	O18–O4 ^{vii}	3.360 (19)
O7–O21	2.66 (4)	O19–O12	2.731 (17)
O7–O21 ^{xi}	2.66 (5)	O19–O18 ^{xii}	2.860 (18)
O7–O18 ^x	3.167 (19)	O19–O4 ^x	2.959 (16)
O7–O20 ^x	3.23 (2)	O19–O19 ^{viii}	3.12 (3)
O8–O17 ^{xi}	2.833 (18)	O19–O2 ^{viii}	3.174 (17)
O8–O20 ^{iv}	3.11 (2)	O19–O16	3.186 (19)
O8–O20 ^x	3.184 (19)	O19–O6	3.397 (18)
O10–O18 ^{xii}	2.727 (18)	O20–O11 ^{vii}	2.75 (2)
O11–O20 ^x	2.75 (2)	O20–O21 ^{vii}	2.76 (4)
O12–O19	2.731 (17)	O20–O17 ⁱⁱ	3.052 (19)
O13–O17 ^{vi}	2.849 (17)	O20–O8 ⁱ	3.11 (2)
O14–O16	2.922 (12)	O20–O8 ^{vii}	3.184 (19)
O15–O17 ^{xiii}	2.955 (17)	O20–O7 ^{vii}	3.23 (2)
O16–O14 ^{viii}	2.922 (12)	O18–O20	3.23 (2)
O16–O14	2.922 (12)	O21–O7 ^{xi}	2.66 (5)
O16–O4 ^{vii}	2.987 (12)	O21–O7	2.66 (4)
O16–O4 ⁱⁱⁱ	2.987 (12)	O21–O20 ^x	2.76 (4)
O16–O17 ^{xiii}	3.130 (18)	O21–O18 ^x	2.77 (4)
O16–O17 ⁱ	3.130 (18)	O21–O1 ^x	3.12 (4)
O16–O19 ^{viii}	3.186 (19)	O21–O5 ^{xi}	3.26 (4)
O16–O19	3.186 (19)	O21–O2 ^{xv}	3.30 (4)

Symmetry codes: (i) $-x + \frac{1}{2}, y + \frac{1}{2}, z$; (ii) $-x + \frac{1}{2}, -y + \frac{3}{2}, z + \frac{1}{2}$; (iii) $-x + \frac{1}{2}, -y + \frac{3}{2}, z - \frac{1}{2}$; (iv) $-x + \frac{1}{2}, y - \frac{1}{2}, z$; (v) $x, -y + 1, z - \frac{1}{2}$; (vi) $x, -y + 1, z + \frac{1}{2}$; (vii) $x - \frac{1}{2}, -y + \frac{3}{2}, -z + 1$; (viii) $-x, y, -z + \frac{1}{2}$; (ix) $x - \frac{1}{2}, y - \frac{1}{2}, -z + \frac{1}{2}$; (x) $x + \frac{1}{2}, -y + \frac{3}{2}, -z + 1$; (xi) $-x + 1, y, -z + \frac{1}{2}$; (xii) $-x, -y + 1, -z + 1$; (xiii) $x - \frac{1}{2}, y + \frac{1}{2}, -z + \frac{1}{2}$; (xiv) $x + \frac{1}{2}, y - \frac{1}{2}, -z + \frac{1}{2}$; (xv) $x + \frac{1}{2}, y + \frac{1}{2}, -z + \frac{1}{2}$.

task for two hydroxyl groups at moderately long distances (2.9 Å). Similarly, the b.v.s. for O13 and O15, which also share an accepting water molecule, are at the bottom end of the range found. The use of two water molecules as acceptors for two hydroxyl groups, rather than that required from the compound stoichiometry, leaves one water molecule oxygen, O21, free of interactions with the uranium oxygen layers, except in terms of a donor function to the uranyl O atoms. This hydrogen-bonding arrangement is discussed further below.

4.2. Water molecule layers

In terms of the formulae the only difference between schoepite and *meta*-schoepite is eight molecules per unit cell. By consideration of the hydrogen-bonding schemes Finch *et al.* (1998) predicted the loss of the water molecule containing his W(5) and W(11) (highlighted in Fig. 4) as these units cannot be tetrahedrally coordinated, in terms of four donor or acceptor functions, in schoepite. However, the actual arrangement of the water molecules in *meta*-schoepite shows

Table 7

Bond-valence arrangement in *meta*-schoepite.

	U1	U2	U3	U4	Sum
O1		2.08			
O2			1.70		
O3	1.99				
O4		1.88			
O5			1.90		
O6				1.85	
O7	1.94				
O8				1.74	
O9		0.74	0.69	0.74	2.17
O10	0.48	0.38		0.54	1.40
O11	0.50	0.49		0.54	1.50
O12	0.41		0.49	0.45	1.35
O13		0.48	0.45	0.39	1.32
O14	0.49	0.47	0.35		1.31
O15	0.62		0.60		1.22
Total	6.42	6.52	6.18	6.22	

that the transformation of the crystal structure is rather more complicated than the simple removal of specific water molecules. Not unexpectedly, the complete water sublattice and to some degree the orientations of the uranyl groups shift to accommodate the lower level of water.

Consideration of the water molecule layers in the two structures show that some correspondence exists and the structures can be related by partial removal of oxygen water molecules from certain sites within the schoepite layers. However, the symmetries of schoepite ($P2_1ca$) and *meta*-schoepite ($Pbcn$) are such that it is not possible to develop a model that simply removes individual water molecules from one structure to obtain the other.

Fig. 4 demonstrates how some water molecules may be removed and others slightly shifted so as to transform schoepite to *meta*-schoepite. Within the unit cell, outlined removal of the highlighted O atoms [W(1) and W(7) in Finch *et al.*'s, 1998) description] and replacement of four O atoms [W(9), W(10), W(3) and W(4)] by the half-filled sites close to (0.5,0.75,0.29) results overall in the removal of four water molecules in the unit-cell layer, consistent with the formulae $(UO_2)_4O(OH)_6 \cdot 6H_2O$ and $(UO_2)_4O(OH)_6 \cdot 5H_2O$. The small shifts that occur in the remaining oxygen positions produce a new hydrogen-bonded network. The potential interactions in the new hydrogen-bonded network are summarized in Table 6 and shown for each of the six water molecule environments in detail in Figs. 5(a)–(f) (deposited).¹

For the partially occupied water oxygen site, O21W, consideration of the higher-symmetry adjacent symmetric site at (0.5,0.75,0.25), that this water molecule might be expected to occupy, shows that an overly short distance to O7 (uranyl oxygen) of 2.54 Å would be obtained. By displacing this atom to the refined position this interaction is extended to a much more reasonable 2.69 Å, while maintaining reasonable hydrogen-bonding links to all other acceptor/donor O atoms.

¹Supplementary data for this paper are available from the IUCr electronic archives (Reference: CF0009). Services for accessing these data are described at the back of the journal.

5. Conclusions

The structure of *meta*-schoepite consists of layers of identical composition to those of schoepite, and water molecules are removed and relocated within the interleaved sheets so as to form a new hydrogen-bonded array.

The lattice parameter changes that occur in the schoepite to *meta*-schoepite have been reported as 14.337 to 13.99, 16.813 to 16.72 and 14.731 to 14.68 Å. Room-temperature values for the *meta*-schoepite material studied in this work were 14.050 (2), 16.709 (2) and 14.7291 (2) Å. The values of the lattice parameters found in this study at 150 K show a distinct contraction on cooling in the *a* and *c* directions to 13.980 (1) and 14.686 (1) Å (these are *b* and *a*, respectively, using the standard *Pbcn* description used in this work), but little change in *b* [16.706 (1) Å, equivalent to *c* in this work]. The main contraction between schoepite and *meta*-schoepite is in the direction perpendicular to the plane (2.8% compared with 0.6 and 0.9% in the other directions). This presumably reflects an improved registration of the water molecule and uranium oxide hydroxide sheets, and the bridging of the sheets by the dual acceptor nature of the two water molecules.

The ease of dehydration and rehydration of phases in the *meta*-schoepite system has been discussed by Finch *et al.* (1998) and similar effects were observed in this study. Several crystals of *meta*-schoepite were investigated during this study and were found to adopt the crystal structure described in this article. One crystal, which had been cooled to 150 K, allowed to warm to room temperature and then left under ambient conditions, was studied again several months later. This crystal had undergone a transformation to a material of the composition $(\text{UO}_3)_4 \cdot 9\text{H}_2\text{O}$ or $\text{UO}_3 \cdot 2.25\text{H}_2\text{O}$, space group *Pbna*, *a* = 15.143, *b* = 14.112, *c* = 16.768 Å (at 150 K). A further crystal

from the original batch, which had been stored under ambient conditions, was found to have the composition $(\text{UO}_3)_4 \cdot 8.5\text{H}_2\text{O}$, space group *Pbcn*, *a* = 14.627, *b* = 14.031, *c* = 16.702 Å (at 150 K). It is clear that additional structural and compositional complexities exist in the $\text{UO}_3 \cdot (2 \pm x)\text{H}_2\text{O}$ system and we intend to report these in a later article.

We thank Professor M. B. Hursthouse for access to the Enraf–Nonius Kappa CCD diffractometer.

References

- Billet, V. & de Jong, W. F. (1935). *Natuurwet. Tijdschr. Ned. Indie*, **17**, 157–162.
- Brown, I. D. & Altermatt, D. (1985). *Acta Cryst.* **B41**, 244–247.
- Brown, I. D. & Wu, K. K. (1976). *Acta Cryst.* **B32**, 1957–1959.
- Christ, C. L. & Clark, J. R. (1960). *Am. Mineral.* **45**, 235–239.
- Debets, P. C. & Loopstra, B. O. (1963). *J. Inorg. Nucl. Chem.* **25**, 945–953.
- Finch, R. J., Cooper, M. A., Hawthorne, F. C. & Ewing, R. C. (1996). *Can. Mineral.* **34**, 1071–1088.
- Finch, R. J., Hawthorne, F. C. & Ewing, R. C. (1998). *Can. Mineral.* **36**, 831–845.
- Hoekstra, H. R. & Siegel, S. (1973). *J. Inorg. Nucl. Chem.* **35**, 761–779.
- Hooft, R. (1998). *Collect. Nonius BV*, The Netherlands.
- Otwinowski, Z. & Minor, W. (1997). *Methods in Enzymology*, Vol. 276, *Macromolecular Crystallography*, Part A, edited by C. W. Carter Jr and R. Sweet, pp. 307–326. New York: Academic Press.
- Piret, P. (1985). *Bull. Miner.* **108**, 299–304.
- Schoep, A. (1932). *Mus. Congo Belg. Ann. Miner. I Fasc.* **III**, 5–7.
- Schoep, A. & Stradiot, S. (1947). *Am. Mineral.* **32**, 344–350.
- Sheldrick, G. M. (1990). *Acta Cryst.* **A46**, 467–473.
- Sheldrick, G. M. (1997). *SHELXL97*. University of Göttingen, Germany.
- Walker, T. L. (1923). *Am. Mineral.* **8**, 67–69.